Appl. Phys. B 62, 465–471 (1996)

Applied Physics B Lasers and Optics

Birth and evolution of wave-front dislocations in a laser beam passed through a photorefractive $LiNbO_3$: Fe crystal

A. V. Ilyenkov, A. I. Khiznyak, L. V. Kreminskaya, M. S. Soskin, M. V. Vasnetsov

Institute of Physics, National Academy of Sciences of Ukraine, Prospect Nauki 46, 252650 Kiev 22, Ukraine
(E-mail: SOSKIN@oqe.ip.kiev.ua)

Received: 7 July 1995/Accepted: 5 October 1995

Abstract. We report on an experimental and numerical investigation of the process of spontaneous optical vortices nucleation in a wave front of a laser beam passed through a photorefractive $LiNbO_3$: Fe crystal with self-induced nonlinear lens. The complex lens structure produces mainly defocusing of the beam passing through the crystal due to a negative variation of the refractive index, whereas side parts of the lens have a positive sign of refractive-index variation and partially focus the beam. The resulting wave-front distortions lead to a phase bifurcation occurring at a certain distance after the crystal when the amplitude of the light wave becomes zero. We study in detail the process of edge dislocation nucleation and its decay in the near field producing a pair of unity-charged opposite-sign screw dislocations. After birth, they spread along dislocation axes as stable objects.

PACS: 42.65

The new area in optics dealing with optical vortices, or screw dislocations in wave fields, attracts now a growing interest. Optical vortices, which look like "dark beams" embedded in light waves, demonstrate interesting behavior in linear and nonlinear optics [1–14].

It was shown that a wave front, usually supposed to be a continuous smooth surface, can be torn under the effect of the tension caused by phase distortions, thus producing phase singularities on the wave front and "helical stairway" around them connecting neighboring 2π-separated wave fronts. The resulting wave-front structure contains optical vortex which is a phase defect, or screw dislocation with zero-intensity line at the center of a dislocation.

The origin of screw dislocations is easily observable in a speckle field of coherent light scattered by a diffuser [2]. Another way to obtain a wave with screw dislocations is to use active systems: lasers operating on several transverse modes [3–5] and photorefractive oscillators [6] or phase-reversal mirrors [7]. In these systems, the nucleation of a pair of vortices (with opposite topological charge) can be described as a phase bifurcation on a wave front due to the interference of transverse cavity modes [7]. In a regular optical wave, it is possible to create a single screw dislocation using spiral Fresnel zone plate [8], binary synthesized diffraction gratings [9, 10], or helical phase converter [11, 12]. The propagation of optical vortices in free space and nonlinear medium was also investigated in theory and experiments [13–17].

The question under test is the process of dislocations originating in a light wave interacting with a nonlinear medium in systems without feedback and determined cavity modes. In our previous publications [18, 19] we demonstrated the spontaneous birth of a "quadruple" of screw dislocations in a beam distorted by the nonlinear self-action in a photorefractive crystal. The aim of the work is to investigate theoretically and experimentally a scenario of the screw dislocation nucleation in a wave front of a wave passed through nonlinear photorefractive $LiNbO_3$: Fe crystal.

1 Theory and calculations

In this paper, we describe the transformations of a wave-front shape due to nonlinear phase distortions caused by the self-action of a beam passing through a photorefractive crystal. The calculations are based on a physical model of a stationary nonlinear lens occurring in a photorefractive crystal with a local nonlinear response. When a crystal is illuminated by a Gaussian laser beam, excited photoelectrons redistribute inside its volume, thus producing refractive-index variation via electro-optic effect. The main photoelectron motion is directed along the C-axis of the crystal from the area of maximum illumination toward dark regions. This determines the lens structure which distorts the beam mostly in the direction parallel to the C-axis of the crystal.

The effect of a beam distortion in photorefractive media, the so-called optical damage, is well known since 1966 [20], and it is usually reputed as a harmful phenomenon. In addition to the nonlinear lens formation, strong

scattering occurs in the process of optical damage due to the recording of photorefractive noise gratings.

Recent papers [21, 22] were devoted to the explanation of the self-defocusing caused by optical damage and the structure of a nonlinear lens induced in a crystal. The detailed mathematical model of the induced lens was proposed in [21]. We took this analysis as a basis for our calculations of a wave-front shape of a beam transmitted through the lens. In x, y coordinates, where the x-axis is directed along the C-axis, the variation of the refractive index $\Delta n(x, y)$ for the polarization of light being parallel to the C-axis has a form (with the induced lens assumed to be thin):

$$\Delta n(x, y) = (\alpha/r^2)\{[1 - \exp(-r^2/w^2)](1 - 2x^2/r^2) + (2x^2/w^2 + Qr^2x/w^3)\exp(-r^2/w^2)\}, \quad (1)$$

where $r = \sqrt{x^2 + y^2}$, α is a normalized magnitude of index variation, w is the radius of a laser beam waist, Q is a parameter of lens asymmetry conditioned by a physical type of nonlinear response: for pure local response $Q = 0$ and in the case of non-local response $Q > 0$. Figure 1 shows a 3D view of the refractive-index variation with a central minimum (negative lens) and side maxima (positive lenses) for the cases of asymmetrical and symmetrical lenses.

Spatial evolution of a beam passed through a photorefractive crystal with induced nonlinear lens was numerically simulated. The nonlinear lens works as a thin phase transparent:

$$\Delta\Phi(x, y) = -2\pi d\Delta n(x, y)/\lambda, \quad (2)$$

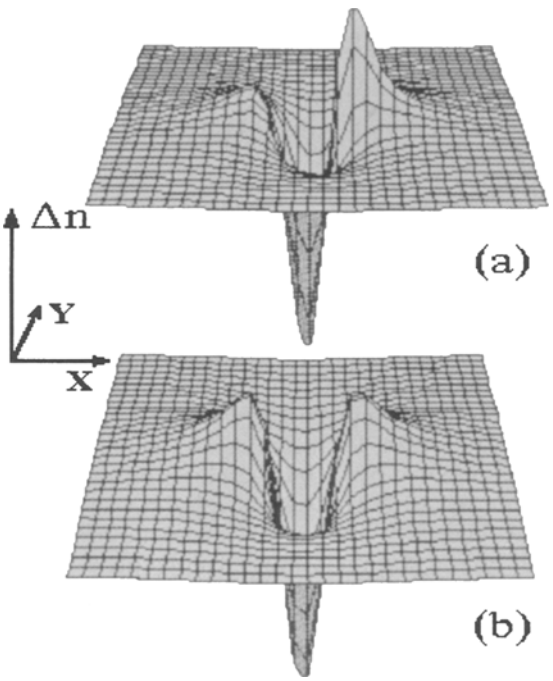

Fig. 1a, b. Refractive-index variation due to nonlinear lens formation in a photorefractive crystal: (**a**) general case, with both local and non-local components of nonlinear response, $Q = 2$, (**b**) symmetrical lens, with pure local response, $Q = 0$

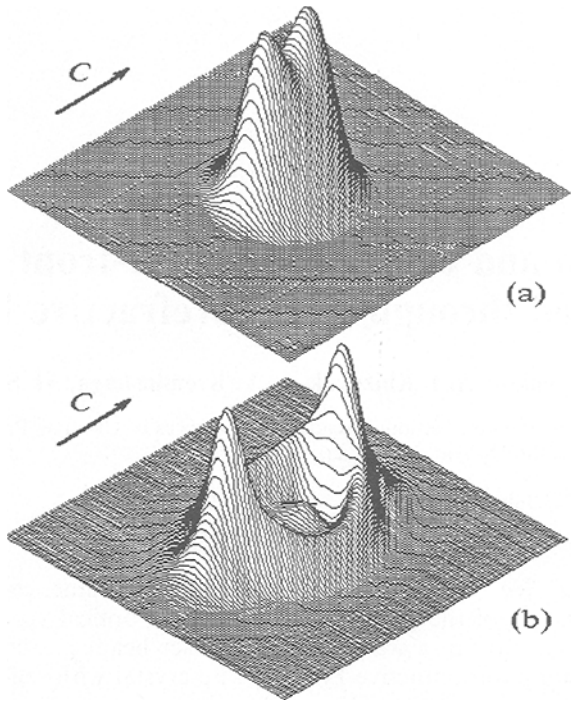

Fig. 2a, b. Calculated intensity distributions in a beam passed through a photorefractive crystal with self-induced nonlinear lens: (**a**) distortion along the C-axis, with central minimum, (**b**) central crater with two extended minima oriented perpendicular to the C-axis

where d is the crystal thickness, λ is the wavelength of the beam. This transparent is located in the waist of the incident Gaussian beam $I(r) = I_0 \exp(-r^2/w^2)$. In order to calculate the distribution of the light-wave intensity in a plane $z = \infty$, spatial Fourier transform was used. The crystal parameters, wavelength λ and the beam radius w were chosen in correspondence with real experiment. We consider the symmetrical case first: $Q = 0$. Then all calculated values have symmetrical distributions with respect to the x and y axes.

The intensity distributions were calculated also at different distances z_0 from the phase transparent for progressively increasing lens strength which is characterized by the maximum value $\Delta\Phi_m = \Delta\Phi(x = 0, y = 0)$. Figure 2 exhibits the distributions obtained for a far-field zone. At first ($\Delta\Phi_m = 0{,}8\pi$), the beam enlarges mainly along the C-axis and an intensity hollow is formed at the beam center (Fig. 2a). Then ($\Delta\Phi_m = 1.6\pi$), this intensity gap acquires the form of a crater with two extended minima oriented perpendicular to the C-axis (Fig. 2b). The wave-front dislocations are formed just in these minima where the intensity vanishes.

Obtained intensity distributions of transmitted beam, however, do not explain the mechanism of a wave-front dislocation birth. To have phase portraits of a wave front, we calculate the following two functions, namely the real and imaginary parts of the complex amplitude $E(x, y, z)$: $\mathrm{Re}\{E(x, y, z = z_0)\}$ and $\mathrm{Im}\{E(x, y, z = z_0)\}$, for different values of $\Delta\Phi_m$. In the plane $z = z_0$, equiphase lines $\mathrm{Re}\{E(x, y, z = z_0)\} = 0$ and $\mathrm{Im}\{E(x, y, z = z_0)\} = 0$ are

plotted to find the dislocation points as points of intersections of these lines. The behavior of equiphase lines may be determined by a simple description for these functions:

$$\begin{aligned} \mathrm{Re}\{E(x,y,z_0)\} &= |E(x,y,z_0)|\cos\Phi(x,y,z_0), \\ \mathrm{Im}\{E(x,y,z_0)\} &= |E(x,y,z_0)|\sin\Phi(x,y,z_0), \end{aligned} \tag{3}$$

where the absolute phase Φ is a function of transverse coordinates and longitudinal propagation. Choosing equiphase wave-front surface by a condition $\Phi = 2m\pi$ (this condition defines a family of wave-front surfaces, $m = 0, 1, 2 \ldots$), it is possible to describe in space each wave front of the family. To simplify the problem, we suppose $z = z_0 = \text{const}$, and calculate only the cross-section lines of wave fronts by the plane $z = z_0$. Due to the continuity of curved wave-front surface, each cross-section line will be a closed line in a general case, and a system of enclosed equiphase lines corresponding to different m will appear in the plane $z = z_0$. They are separated by 2π, as follows from the wave-front definition. However, absolute phase Φ is determined only with an accuracy of an arbitrary constant, and we may define only relative position of equiphase lines. If we can let the phase be zero (or $2m\pi$) on some equiphase line, we automatically define the position of all lines where $\sin\Phi = 0$, with phase separation π between them (they will be the lines $\mathrm{Im}\{E(x,y,z_0)\} = 0$), and also equiphase lines where $\cos\Phi = 0$ ($\mathrm{Re}\{E(x,y,z_0)\} = 0$). The phase separation between thus defined neighboring equiphase lines $\mathrm{Im}\{E\} = 0$ and $\mathrm{Re}\{E\} = 0$ is $\pi/2$. For identical wave fronts following each other, these lines are the projections of a single wave-front equiphase lines $\Phi(x,y,z_0 + m\lambda) = \text{const}$ on the plane $z = z_0$. It means that instead of the calculation of all points of a wave-front surface, we only calculate projections of equiphase lines on a plane $z = z_0$. The distance between equiphase lines on this plane will be larger when the wave front approaches nearly plane wave, condensation of the lines indicates that there is a fold on the wave front. If neighboring lines $\mathrm{Im}\{E\} = 0$ and $\mathrm{Re}\{E\} = 0$ touch each other at some points, the only one solution following from (3) is $E(x_0, y_0, z_0) = 0$. The location of zero-amplitude point does not depend on the choice of the absolute phase, and an important consequence is that the points of intersection of the equiphase lines will be the same whatever phase was attributed to the selected reference line. The same is valid for the intersection points. The intersection of equiphase lines means that the wave fronts with neighboring m $(m, m+1)$ are connected, producing screw dislocation around the dislocation axis crossing the plane $z = z_0$ at a point x_0, y_0. The more interesting feature is that there is a distance z_n from the crystal where dislocation should nucleate: no dislocations are present in a wave for $z < z_n$ and a dislocation pair is expected to exist at $z > z_n$. Further, we shall discuss a phase bifurcation which leads to dislocation pair birth, and now we start to describe the calculations of phase distributions in a far-field zone.

For small values of the lens strength, $\Delta n \cong 0$, equiphase lines are nearly concentric circles. The subsequent growth of the lens strength causes deformations of the equiphase lines (Fig. 3a) without their intersections until $\Delta\Phi_m < 1.6\pi$. For $\Delta\Phi_m < 1.6\pi$, the two lines $\mathrm{Re}\{E\} = 0$ and $\mathrm{Im}\{E\} = 0$ touch each other and produce

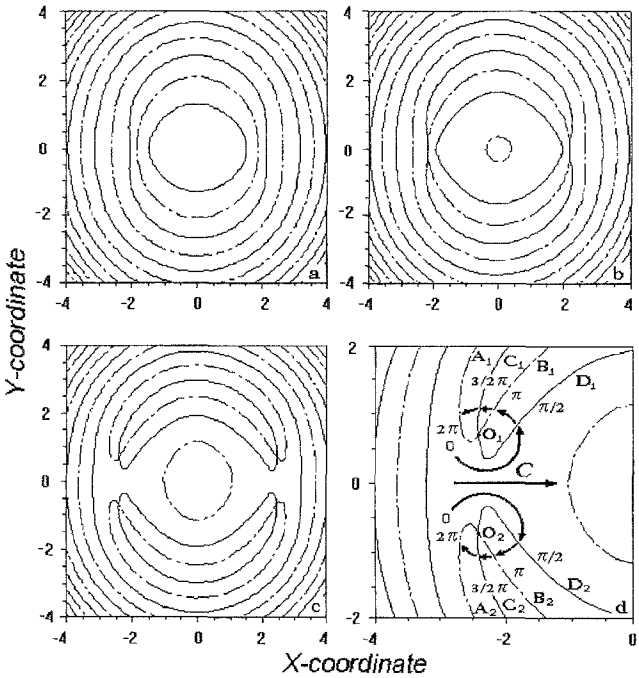

Fig. 3a–d. Calculated equiphase lines $\mathrm{Re}\{E\} = 0$ and $\mathrm{Im}\{E\} = 0$ in a far-field beam cross section for different values of nonlinear lens strength (**a**, **b**, **c**). Two phase singularities on a phase map (c) at the points O_1 and O_2 are shown with magnified scale (**d**)

two definite zero-amplitude segments oriented perpendicular to the C-axis (Fig. 3b). Phase jumps by π at these segments. It means that two limited edge dislocations are formed. Further small increase of the lens strength up to $\Delta\Phi_m = 1.62\pi$ gives the intersections of the lines in four points which correspond to four screw wave-front dislocations origin (Fig. 3c), i.e. each of these two edge dislocations decays on two pairs of screw dislocations with opposite signs. The orientation of pairs is also opposite. Thus a "quadruple" of screw dislocations is formed in the beam wave front. Phase map of Fig. 3d may be used for the determination of each dislocation sign. The selected lines, $\mathrm{Re}\{E\} = 0$ and $\mathrm{Im}\{E\} = 0$, are equiphase lines with phase separation $\pi/2$ between them. At the intersection points O_1 and O_2, phase is undetermined and jumps by π. Close to each intersection point, the selected equiphase lines have phase values 0 (or 2π) (A_1O_1, A_2O_2), π (B_1O_1, B_2O_2), $3\pi/2$ (C_1O_1, C_2O_2), and $\pi/2$ (D_1O_1, D_2O_2). Choosing the direction of rotation from smaller phase value to larger we have a clockwise screw wave-front dislocation at the point O_2 and a counter-clockwise wave-front dislocation at the point O_1, as shown in Fig. 3d. In a local area around the point O_1, the wave front has a form of a left helix, and around the point O_2 it forms a right helix. According to the definition introduced in [23] we may attribute positive sign to the dislocation at point O_2 and negative sign to the dislocation at point O_1.

The screw dislocation quadruple conserves and increases its size with further growth of $\Delta\Phi_m$. At $1.8\pi < \Delta\Phi_m < 2.2\pi$ new concentric lines, $\mathrm{Re}\{E\} = 0$ and $\mathrm{Im}\{E\} = 0$, appear in the beam center inside the quadruple. These lines are bent by the same scenario and at

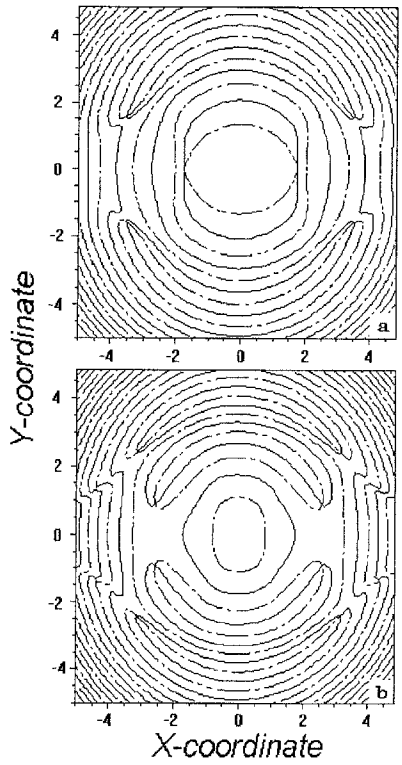

Fig. 4a, b. Calculated equiphase lines $\mathrm{Re}\{E\} = 0$ and $\mathrm{Im}\{E\} = 0$ in a far-field beam cross section for larger lens strength than in Fig. 3; formation of the internal "quadruple" is seen

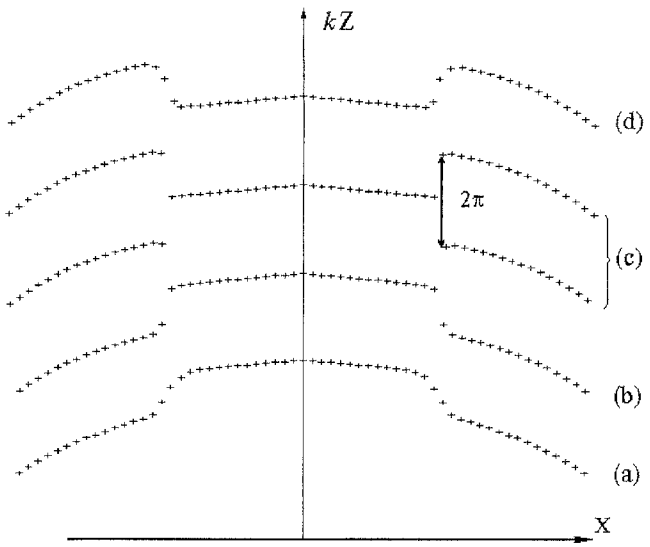

Fig. 5. Calculated wave-front cross section at different distances from a crystal: (*a*) ledge is seen at the apex of the wave front; (*b*) phase step is forming; (*c*) phase step on π tears the wave front; (*d*) wave front restores continuity along *x*-axis, phase defects are out of picture plane, and four screw dislocations are born

$\Delta\Phi_m = 2.24\pi$, two new limited edge dislocations are formed, At $\Delta\Phi_m = 2.28\pi$ they decay on two pairs of screw dislocations forming a new dislocation quadruple inside the large external quadruple. The signs of vortices within both these quadruples are the same (Fig. 4).

With existing dislocations a in far-field zone, it is possible to determine the distance z_n of their origin. The stronger is a nonlinear lens, the smaller is z_n (the plane of dislocation nucleation moves closer to the crystal). We show in Fig. 5 how the wave-front structure changes along the distance from the crystal (k is a wave number $2\pi/\lambda$). Due to the sign of light-induced change of refractive index ($\Delta n < 0$) in the central part of a beam, optical path in the crystal is slightly smaller near the beam apex, and wave fronts produce ledge, as shown in Fig. 5a. Phase step develops on its edge (Fig. 5b) and when the magnitude of the step reaches π (Fig. 5c), phase bifurcation occurs: the phase becomes indeterminate and the wave front tears. Farther central wave-front part joins with a peripheral part of the following wave-front. Then the phase step reverses with respect to the direction of propagation (Fig. 5d), and the wave-front continuity in the *x*-direction restores. Due to the lens asymmetry, the wavefronts has smaller distortions in the *y*-direction and remains continuous along the *y*-axis. This leads to the origin of four phase defects on its surface, which are screw dislocations (vortices). Their signs are determined by negative-type index variation.

The case of asymmetrical lens was also studied numerically. The difference in the process of dislocation birth relative to the symmetrical case is that the nucleation of vortices in the right and left parts of a beam occurs on different distances z_n from the crystal position. Figure 6 shows phase maps in the near-field zone for the case of asymmetric lens ($Q = 2$).

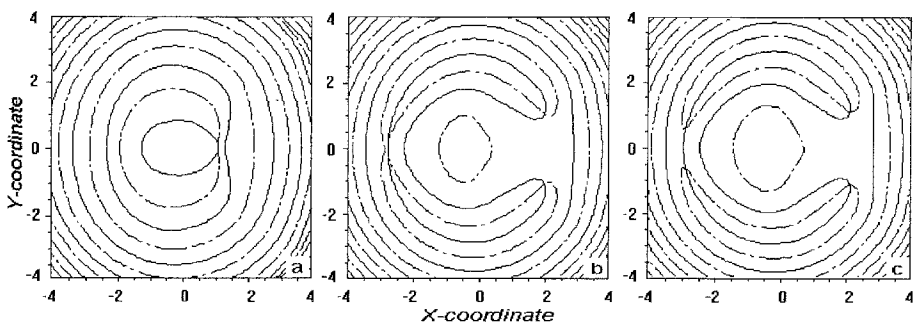

Fig. 6a–c. Calculated equiphase lines $\mathrm{Re}\{E\} = 0$ and $\mathrm{Im}\{E\} = 0$ in a far-field beam cross section for the case of asymmetric lens. First two opposite-sign screw dislocations nucleate at the right side of the beam (**a**, **b**), then at the left side (**c**)

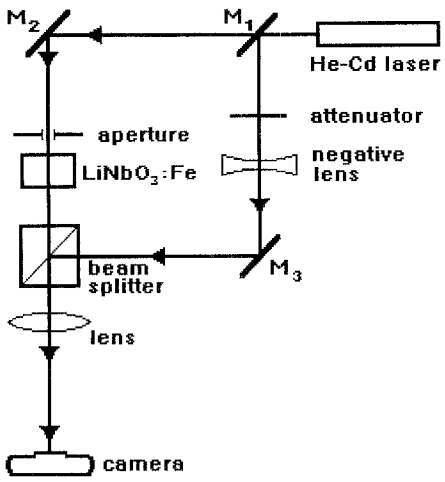

Fig. 7. Experimental setup for investigation of phase defect nucleation in a laser beam distorted by self-induced nonlinear lens in a photorefractive $LiNbO_3$ crystal. M_1 is semi-transparent mirror, M_2 and M_3 are highly reflective mirrors.

2 Experimental

The experimental scheme is shown in Fig. 7. An $LiNbO_3$: Fe crystal was placed in one arm of the interferometer. Polished faces of y-cut were parallel to the C-axis. We tried three crystals with slightly different parameters, with 0.03% weight content of Fe^{3+} ions and thicknesses 3, 4 and 8 mm. A He–Cd laser radiation on the Gaussian mode with beam diameter 1.2 mm (non-focused beam) and linear polarization oriented along the C-axis was directed on the input face. An aperture was placed before the crystal to cut off the scattered radiation. An attenuator and a negative spherical lens were introduced into the referent arm of the interferometer to obtain high-contrast interference pictures. The interferometer arrangement ensures observation and registration of interferograms corresponding to far-field and near-field locations. The angle between reference and tested beams was adjusted to produce horizontal fringes parallel to the C-axis. The proper choice of the angle enables an appropriate fringe spacing and detection of the charge of phase defects: a "fork" orientation toward the C-axis indicates positive sign of a screw dislocation and vice versa [23].

Radiation power was chosen small enough (< 1 mW) that the development time of induced optical inhomogeneities was 10 min which is much longer than the transient time, and allowed to observe all details of intensity and phase distributions in a beam distorted by slowly varying lens. Actually, we do not create steady-state nonlinear lens due to the continuous influence of the laser beam, but we can "freeze" the lens at each moment of exposure by laser power diminishing to the extent suitable only to visualize recorded lens without its further growth.

In experiment, we observed intensity distributions and the corresponding interferograms (dislocation pictures) of transmitted beam in the far field and the near field starting from the output plane of the crystal in different moments of time. The main steps of a beam evolution observed in the far field are shown in Fig. 8. In the beginning of exposure ($t = 0$), nonlinear lens is not formed yet and the transmitted beam has nearly a Gaussian intensity distribution and a smooth wave front. Further lens development distorts a beam forming bright ring with a dark central zone (self-defocusing). After a while ($t = 20$ min) the influence of self-induced lens leads to the origin of two extended intensity gaps oriented perpendicular to the C-axis (Fig. 8a). The picture is slightly asymmetric: this fact testifies the contribution of photoexcited carriers diffusion into optical-damage process, that is mixed type of crystal nonlinear response. Corresponding interferogram in Fig. 8d shows that an edge dislocation nucleates in a right-located gap (positive direction of the C-axis) meanwhile fringes at a left gap are bent, but continuous: phase fold develops along the intensity minimum.

With further increase of the lens optical strength ($t = 25$ min), edge dislocation still exists at the right gap and a second edge dislocation nucleates at the left gap. This means that light intensity in both gaps equals zero on some intervals, which look as black segments in Fig. 8b. Corresponding interferogram (Fig. 8e) shows that interference fringes are broken in these places: a bright fringe turns into a black one and vice versa. This proves the existence of the edge dislocation (phase step on π), which cannot be detected from light-distribution picture itself. The half-forks are seen at the ends of edge dislocation. They are oriented in opposite directions, that is half-forks have topological charges of equal value and opposite signs. As a result, the total topological charge of the limited edge dislocation is zero, in correspondence with topological charge conservation low in free-spreading wave fields (the initial Gaussian beam with vortices-free wave front has zero topological charge).

With consequent increase of nonlinear lens strength ($t = 35$ min), firstly right edge dislocation and then left edge dislocation decays on separate opposite-sign screw dislocations: broken fringes in the middle part of the phase defect connect each other, but with a shift on one fringe. It results in one fringe lack at one end of the gap and one extra fringe at the other end, which forms oppositely directed "forks". Thus both edge dislocations transform into "dipoles" of two isolated screw dislocations which appear at their ends (Fig. 8f). In the intensity picture, separated black points are observed (Fig. 8c). The vortices in these dipoles are oriented in the opposite directions, i.e. "quadruple" of screw dislocations is formed. The distance between vortices in a dipole increases starting from the initial separation which equals the edge dislocation length.

Further ($t = 60$ min) new phase defects in the form of two edge dislocations are created inside the quadruple of screw dislocations (intensity minimum observed at the beam center in Fig. 8c corresponds to the beginning of new edge dislocation pair). They have the same evolution in time and also decay into pairs of opposite-sign screw dislocations, and finally new internal quadruple of screw wave-front dislocations arises inside large quadruple. The dislocation signs in both quadruples are the same. Next development of dislocation array under very strong optical damage has more complicated and non-regular character.

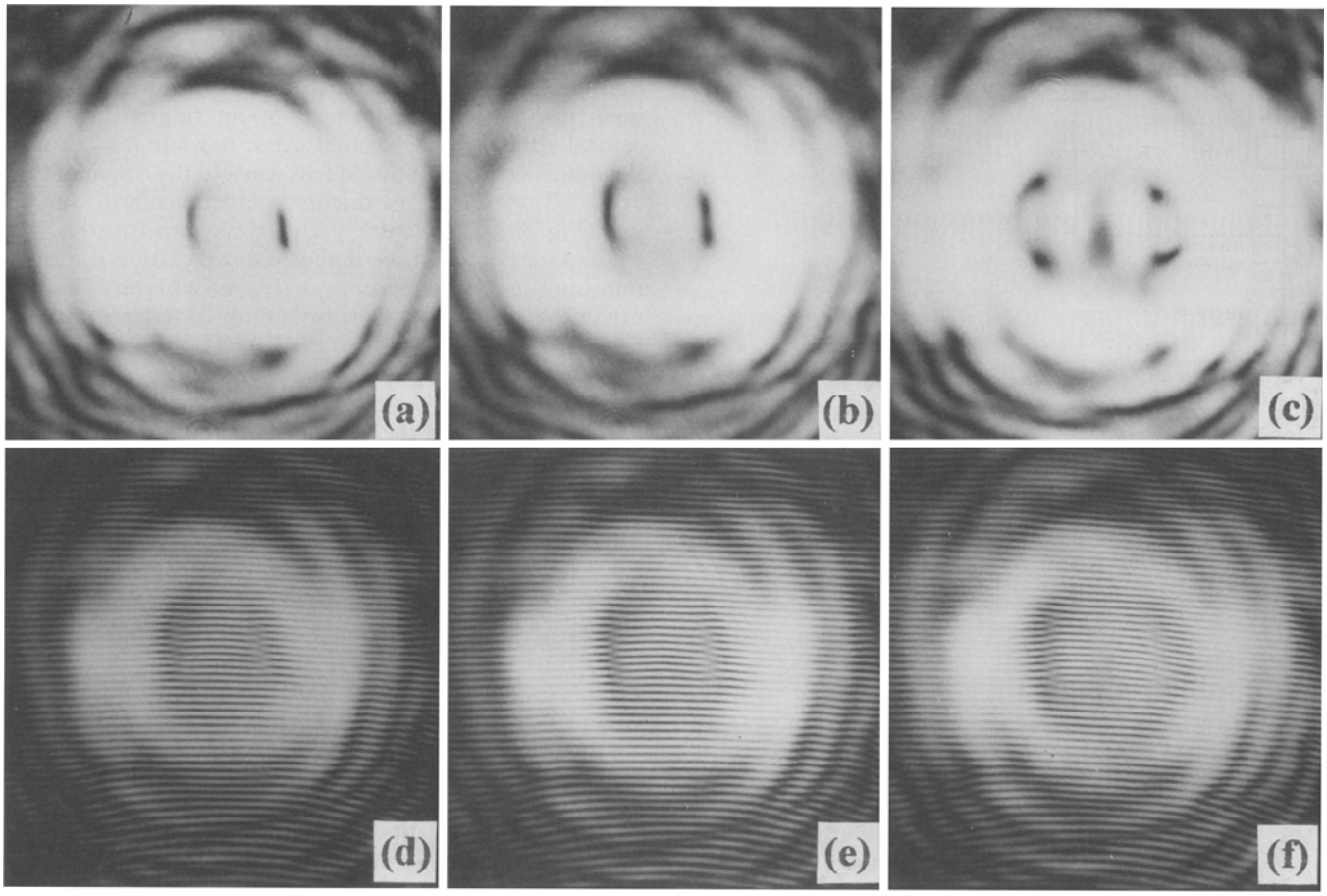

Fig. 8a–f. Far-field view of a beam distorted by optical damage. Early steps of phase defect origin are shown (**a**, **b**, **c**) with corresponding interferograms (**d**, **e**, **f**). The *C*-axis is directed from *left to right*. Asymmetry of the dislocation nucleation is evident: intensity minimum at the right side of the beam is deeper than at the left side (**a**) and edge dislocation is seen at the right gap at first (**d**). Then edge dislocations exist at both sides of the beam (**b**, **e**) and finally four screw dislocations appear (**c**, **f**). Beam divergence is about 4 mrad

The use of an objective lens shown in Fig. 7 permits to observe the creation of dislocations also in the near-field area. We located a plane of edge dislocation nucleation which moves closer to the crystal with the growth of the lens strength, in accordance with the theoretical prediction. We observed the existence of dislocations even inside a crystal when the lens was strong enough. In this case, however, our theoretical model is not valid anymore, because the lens can no longer be treated as thin and the photorefractive response is very different for a beam possessing intensity zeros [24].

3 Discussion and conclusion

The results of our investigations show the mechanism of screw dislocation birth at the process of a wave-front deformation caused by nonlinear lens induced in photorefractive $LiNbO_3$ crystal. The complex lens structure produces defocusing of a beam passing through a crystal due to the negative variation of the refractive index. However, side parts of the lens located along the *C*-axis have positive sign of refractive-index variation and partially focus a beam. The resulting wave-front distortions may lead to a phase bifurcation occurring at a certain distance after a crystal when the amplitude of the light wave becomes zero. We calculate a threshold value of the lens strength which produces, in the far field, nucleation of edge dislocation, according to the used model of the induced lens. We study in detail the process of edge dislocation nucleation and the decay in the near field producing a pair of unity-charged opposite-sign screw dislocations. This process includes the phase bifurcation which is accomplished by the origin of zero-intensity line which corresponds to wave-front local cut with phase step on π between opposite sides of the cut. This wave-front defect is an intermediate state existing in limited distance along the direction of wave propagation and its further transformation creates two separate screw dislocations with opposite helicities. After birth, they spread along the dislocation axes as stable objects.

We note that even in monochromatic wave there is an evolution of a wave-front shape which gives birth to a pair of vortices, so the dislocation axis has a starting point (as follows from [1], dislocation axis should be infinite in both directions in the case of monochromatic wave).

Experimental verification of the theoretical model was found to be in good agreement. Interferometric technique permits to observe phase modulation around lines where light intensity vanishes, and when the amplitude gets zero its phase becomes indeterminate. We observed intensity gap and reversing fringe contrast at this moment. The more interesting point is that zero-intensity area is an extended segment, i.e. there is an interval between two points on the plane $z = z_n$ where $\mathrm{Re}\{E\} = \mathrm{Im}\{E\} = 0$. This is a limited edge dislocation [23], which tends to decay into a pair of screw dislocations appearing on this ends. We detected the connection of broken fringe with shifted one by one spacing at the process of edge dislocation decay, with exact coincidence to the theoretical model predicting the junction of neighboring wave fronts around screw dislocation. However, neither calculations nor experiments could establish yet the extent of edge dislocation along the direction of wave propagation.

Physical mechanism of nonlinear lens development includes a contribution of the photovoltaic effect (local response) and diffusion of photoexcited electrons (nonlocal response). This causes lens asymmetry with respect to the C-axis of a crystal. Both theory and experiment show slight delay of phase defect nucleation between right and left parts of a beam (positive and negative directions of the C-axis), in longitudinal scale in calculations and in time in experiments.

Summarizing, we describe the process of the origin of phase defects in a light wave initially being a Gaussian beam and distorted by self-action in photorefractive crystal, for the first time to our knowledge. Both theoretical calculations and experimental data reveal local cuts of a wavefront (edge dislocations) which decay on pairs of oppositely charged screw dislocations.

Acknowledgements. Authors thank Professor S. G. Odoulov for helpful discussions and for the supply of crystals. This work was supported by International Science Foundation (Grants U61000 and U61200), National Committee of Sciences and Technologies of Ukraine and, in part, by the International Soros Science Education Program (ISSEP, Grant PSU052054).

References

1. J.F. Nye, M.V. Berry: Proc. R. Soc. London A **336**, 165 (1974)
2. N.B. Baranova, A.V. Mamaev, N.F. Pilipetskii, V.V. Shkunov, B.Ya. Zel'dovich: J. Opt. Soc. Am. **73**, 525 (1983)
3. J.M. Vaughan, D.V. Willetts: J. Opt. Soc. Am. **73**, 1018 (1983)
4. C. Tamm, C.O. Weiss: J. Opt. Soc. Am. B **7**, 1034 (1990)
5. P. Coullet, L. Gil, F. Rocca: Opt. Commun. **73**, 403 (1989)
6. F.T. Arecchi, G. Giacomelli, P.L. Ramozza, S. Residori: Phys. Rev. Lett. **67**, 3749 (1991)
7. G. Indebetouw, D. Korwan: J. Mod. Opt. **41**, 941 (1994)
8. N.R. Heckenberg, R. McDiff, C.P. Smith, A.G. Wite: Opt. Lett. **17**, 221 (1992)
9. V.Yu. Bazhenov, M.V. Vasnetsov, M.S. Soskin: JETP Lett. **52**, 429 (1990)
10. N.R. Heckenberg, R. McDuff, C.P. Smith, H. Rubinsztein-Dunlop, M.J. Wegener: Opt. Quantum Electron. **24**, S951 (1992)
11. S.N. Khonina, V.V. Kotlyar, M.N. Shinkaryev, V.A. Soifer, G.V. Uspleniev: J. Mod. Opt. **39**, 1147 (1992)
12. M.W. Beijersbergen, R.P.C. Coerwinkel, M. Kristiensen, J.P. Woerdman: Opt. Commun. **112**, 321 (1994)
13. I.V. Basistiy, V. Yu. Bazhenov, M.S. Soskin, M.V. Vasnetsov: Opt. Commun. **103**, 422 (1993)
14. G. Indebetouw: J. Mod. Opt. **40**, 73 (1993)
15. V.I. Kruglov, Y.A. Logvin, V.M. Volkov: J. Mod. Opt. **39**, 2277 (1992)
16. G. Swartzlander, C. Law: Phys. Rev. Lett. **69**, 2503 (1992)
17. N.N. Rozanov: Opt. Spektrosk. **75**, 861 (1993) (in Russian)
18. M.V. Vasnetsov, A.V. Ilyenkov, M.S. Soskin: Ukrainian Phys. J. **39**, 542 (1994) (in Ukrainian)
19. M. Vasnetsov, A. Ilyenkov, M. Soskin: Tech. Dig. 5th Euroopean Quantum Electronics Conf. (Amsterdam 1994) p. 109
20. A. Ashkin, G.D. Boyd, J.M. Dziedzik, R.G. Smith, A.A. Ballman, K. Nassan: Appl. Phys. Lett. **9**, 72 (1966)
21. V.V. Obukhovskii: Ukrainian Phys. J. **27**, 344 (1982) (in Russian)
22. Q. Wang Song, C. Zhang, P.-J. Talbot: Appl. Opt. **32**, 7266 (1993)
23. I.V. Basistiy, M.S. Soskin, M.V. Vasnetsov: Opt. Commun. **119**, 604 (1995)
24. V. I. Vinokurov, V. V. Shkunov: Kvantovaya Elektron. **16**, 1424 (1989) (in Russian)